Density Functional Study of the Dissociative Adsorption of Aromatic Molecules on the Si(100) Surface: On the Way from Benzene to Larger Polycyclic Hydrocarbons

Francesca Nunzi,*,† Antonio Sgamellotti,† and Nazzareno Re*,‡

Istituto di Scienze e Tecnologie Molecolari (ISTM-CNR) c/o Dipartimento di Chimica Università di Perugia, I-06123 Perugia, Italy, and Facoltà di Farmacia, Università G. D'Annunzio, I-66100 Chieti, Italy

Received: April 10, 2006; In Final Form: November 2, 2006

Density functional calculations have been performed on possible mechanisms for the hypothetic C−H bond cleavage process of benzene chemisorbed on the Si(100) surface, in order to shed light on the analogous process on larger polycyclic aromatic hydrocarbons. We first identified the minima on the potential energy surface for the benzene adsorption on Si(100) and for the breaking of two C−H bonds, with formation of two Si−H bonds, and then we analyzed possible pathways for the C−H bond cleavage, looking for the transition states connecting the adsorption configurations to the final products of C−H breaking. We identified two adsorbed configurations of benzene from which the breaking of two C−H bonds can be accessible, i.e., the 1,2 tilted di-σ bonded configuration on top of a single dimer (**T**) and the 1,4 di-σ bonded configuration where benzene bridges two dimer rows (**BR**). The kinetically most favorable reactive channel on the **T** configuration involves the abstraction of two hydrogen atoms on the sp^3 carbon atoms by the silicon atoms of an adjacent dimer, with an energy barrier of 22.0 kcal mol^{-1}. Although seemingly low, such an activation energy is not expected to be accessible at temperatures below the onset of benzene desorption from this configuration, which requires 15.9 kcal mol^{-1}. The kinetically most favorable reactive channel on the **BR** configuration, which has not been experimentally detected for the benzene molecule, involves the rupture of one Si−C bond, passing through an energy barrier of 29.8 kcal mol^{-1}, and ends with the formation of a Si−H bond and a vertical phenyl unit anchored on a silicon dimer.

Introduction

There is rapidly growing interest in the functionalization of silicon surfaces in view of the development of new nanoelectronics devices.[1−4] Several reactions and techniques for forming bonds between organic molecules and a silicon surface are already well established and have been used in the past few years to modify silicon semiconductor materials. Of particular interest is the reactivity of Si(100) surfaces which are the starting point for most of the integrated circuits used in microprocessors and memory chips.

The Si(100) surface undergoes 2×1 reconstruction where two silicon atoms pair together into dimers. The bonding within these dimers has been described in terms of a strong σ bond and a weak π bond and is therefore electronically similar to C═C or Si═Si double bonds of alkenes or disilylenes.[5] However, the π bond in Si(100) is rather weak, suggesting that a diradical description, each Si atom having an unpaired electron, could be also plausible.[6] In addition, the silicon−silicon dimers may tilt on the surface imparting a zwitterionic character which arises from a charge transfer from the "down" atom to the "up" atom.[7] The buckling of the surface dimers is still a question that continues to be discussed, and considerable controversy remains in both experimental and theoretical aspects. Although the overwhelming experimental evidence indicates that the dimers are buckled at low temperatures,[7a] in agreement with DFT calculations on model clusters, recent higher level multireference perturbation and CCSD(T) calculations show that buckling does not occurr.[7b] However, these calculations are performed on clusters of finite size, and it is not clear to what extent their results can be extrapolated to the bulk. Moreover, the low buckling frequencies[7b] (of the order of 100−200 cm^{-1}) suggest that any asymmetric attack on the surface by a substrate will be likely to cause buckling, so that chemistry that occurs on the surface may be somewhat independent of the exact structure of the considered cluster models. The final reconstructed surface consists of rows of silicon dimers and provides a uniform, ordered, and reactive template for surface chemistry. The reactivity of these silicon dimers with unsatured bonds has been known for several years. In contrast to adsorption at many metal surfaces, adsorption of unsaturated hydrocarbons on Si(100) is often nondissociative and involves interactions via the π bonds in the molecule, leading to the formation of new Si−C σ bonds.[8−11]

Several experimental and theoretical investigations have shown that simple alkenes[12−15] and alkynes[16−18] react through [2+2] cycloaddition, while conjugated dienes molecules react through [4+2] cycloaddition,[19−25] both reactions leading to the formation of two strong Si−C σ bonds. The adsorption of unsaturated aromatic hydrocarbons on the Si(100) surface is a topic of great current interest,[26−34] and the reaction of benzene, the simplest aromatic molecule, is particularly studied. Although some issues regarding the adsorption of benzene on Si(100) are still not clearly understood, the overall picture is quite clear.

On the basis of a combined study using high-resolution electron-energy-loss spectroscopy (HREELS), thermal desorp-

* To whom correspondence should be addressed. E-mail: nunzi@thch.unipg.it (F.N.); nre@unich.it (N.R.) Fax: +39 0755855606 (F.N.); +39 08713555267 (N.R.).

† Istituto di Scienze e Tecnologie Molecolari (ISTM-CNR).

‡ Università G. D'Annunzio.

10.1021/jp062215m CCC: $37.00
Published on Web 12/14/2006

tion spectroscopy (TDS), and Auger electron spectroscopy (AES), Taguchi et al.[26] demonstrated that benzene chemisorbs molecularly on Si(100) at room temperature, and thus proposed that benzene is di-σ bonded to two Si atoms of a dimer on the surface through [2+2] and [4+2] cycloaddition products. On the other hand, scanning tunneling microscopy (STM) studies at room temperature by Lopinski et al.[27−29] have revealed the presence of multiple configurations which, with the help of ab initio calculations, were identified as 1,4 di-σ bonded on top of a single dimer (butterfly configuration, **Bf**) and two different tetra-σ bonded geometries bridging two dimers with a "tight bridge" (**TiB**) and a "twisted bridge" (**TwB**) configuration. Their Hartree−Fock and density functional theory (DFT) calculations showed the **TiB** tetra-σ bonded configuration to be lower in energy than the **Bf** di-σ bonded one. In addition, the STM experiments identified the single-dimer geometry as a metastable precursor to the bridging configurations involving two adjacent Si surface dimers. Further first principle theoretical calculations on the adsorption of benzene on the Si(100) surface have confirmed that the most stable configuration is the tetra-σ bonded **TiB** structure.[30]

The results of vibrational infrared (IR) spectroscopy and near-edge X-ray absorption fine structure (NEXAFS) studies of chemisorbed benzene at 100 K and at room temperature were consistent with the chemisorption of benzene forming a di-σ bonded structure.[31] Moreover, latest experimental[32−34] and theoretical calculations[35] consistently predict the di-σ bonded product to be the lowest energy species and the only reaction product for benzene on the Si(100) surface at saturation coverage and room temperature, pointing out how the use of different experimental tools generated different results and even similar STM techniques can be interpreted differently.

In spite of the unclear identification of the lowest energy configuration, the main features of the adsorption of benzene on the Si(100) surface are quite well understood. In particular, the adsorption is nondissociative, and benzene adsorbs and desorbs almost reversibly: the bond breaking of C−H bonds, which would be easily highlighted by the emergence of a Si−H stretching mode in the IR spectrum, has never been observed.

However, some recent experimental studies gave evidence for the C−H bond breaking in substituted benzenes or larger polycyclic aromatic hydrocarbons. For instance, the Fourier transform IR investigation of styrene adsorption on Si(100) surface has indicated the breaking of a phenyl C−H bond with the formation of Si−H bonds at temperatures above 700 K.[36] A C−H bond breaking has also been observed upon annealing of adsorbed chlorobenzene molecules.[37−38] Pentacene undergoes some C−H bond cleavage from C atoms in the fused ring system; this cleavage results in nearly irreversible adsorption of the pentacene species to the Si(100) surface.[39−42] All this evidence indicates that the C−H bond breaking on a benzene ring upon the adsorption of aromatic hydrocarbons on silicon surfaces is a feasible process at accessible temperatures and suggests that the reason why it has never been observed for simple benzene lies in the easy thermal desorption of this molecule at temperatures below those required to overcome the energy barrier for this breaking process. Indeed, the weakening of the C−H bond due to substituents on the benzene ring would lower the energy barrier for the dissociation process, while the stronger adsorption energy in large polycyclic aromatic molecules such as pentacene, due to a major number of surface Si−C bonds, hinders the desorption process, so that a dissociative event involving the rupture of some C−H bonds becomes feasible at high temperatures.

A speculative theoretical study of the mechanism through which this bond breaking could occur in benzene would therefore be useful to shed light on this hypothetical process and as a guideline to understand the C−H bond breaking in more complex aromatic systems. Indeed, since the parameters controlling the adsorption process of polycyclic aromatic hydrocarbons and benzene on the silicon surface are expected to be very similar except for an energy factor related to the number of benzene units, a theoretical study that analyzes the possible mechanisms for the C−H bond cleavage process on the benzene adsorbed on Si(100) can give useful information for the analogous process for the more complex molecules. To our knowledge, only one semiempirical study has been performed on the adsorption of benzene on Si(100) considering the possibility of a dissociative adsorption, showing that this configuration is less stable in energy than intact chemisorbed configurations.[43]

Here we report a DFT investigation of the possible pathways for the C−H bond breaking following the adsorption of benzene on the Si(100) surface. Geometry optimizations have been performed to characterize the products for the benzene adsorption and for the breaking of two C−H bonds, leading to the formation of two Si−H bonds. We also identified the main transition states connecting the adsorption configurations to the final products of the C−H bond breaking.

Computational Details

The Si(100) surface has been modeled by finite cluster models reproducing two dimers either on the same row or on two adjacent rows of the reconstructed 2×1 silicon surface, respectively $Si_{15}H_{16}$ and $Si_{31}H_{32}$. In both cases, the top layer consists of four silicon atoms, representing the two adjacent surface dimers lying in the same row ($Si_{15}H_{16}$) or on two adjacent rows ($Si_{31}H_{32}$) of the surface, while all the remaining subsurface silicon atoms are saturated by hydrogen atoms to avoid dangling bond effects. Although the terminating hydrogen atoms may create a different chemical environment from the actual Si(100)-2×1 surface at the cluster boundary, a recent study on cluster models of various sizes has shown negligible deviations.[44] The adsorption structures involving these two-dimer cluster models have been optimized by imposing geometrical constraints at the third- and fourth-layers substrate atoms,[45] so as to avoid unrealistic widening of the models upon the benzene chemisorption. This is particularly important for the cluster models of two dimers on adjacent rows (see below) for which attaining the expected bulk rigidity would require the inclusion of too many lower layer atoms, making the calculations computationally too heavy. Since constraining part of a cluster model to maintain the rigidity of the bulk can cause some problems in the geometry near the dimer and lead to imaginary frequencies, we did not fix the coordinates of a whole set of atoms in the lower layers, as usually done, but applied softer constraints, fixing the distances between the outer silicon atoms of the third and fourth layers to the values they assume in the bulk. Using these softer constraints on the silicon atoms, and leaving free the saturating hydrogen atoms, allows a partial relaxation of the lower layers, avoiding the problem of imaginary frequencies. Indeed, every optimized minimum showed all real vibration frequencies, while every transition state showed only one imaginary frequency whose normal mode corresponds to the considered reaction coordinate. The frequency analysis on all stationary points shows a few vibrations with real but small frequencies (below 100 cm^{-1}), whose normal modes correspond to the motion of the constrained silicon atoms. The optimized

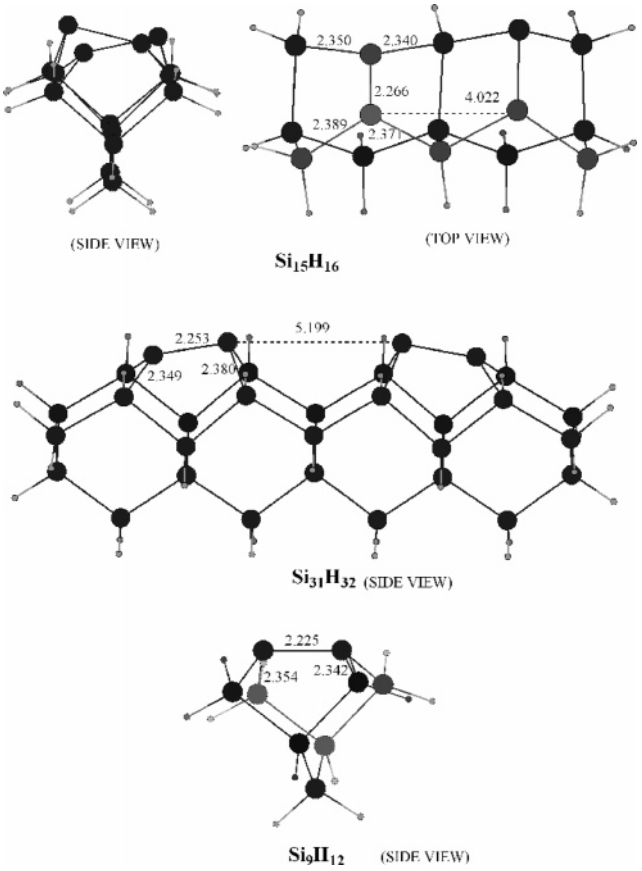

Figure 1. Optimized structures for the employed cluster models of the Si(100) surface, together with the main geometrical parameters (bond lengths in ångstroms).

structures for the bare cluster models described above are reported in Figure 1, together with the dimer Si−Si bond distances and the intradimer Si−Si distances, that will be useful in the following discussion.

In order to reduce the computational cost, a third smaller cluster, the well-known single-dimer Si_9H_{12} model, has been employed in the calculations of the stationary points (minima and transition states) for processes where only one silicon dimer is involved. Its optimized structure is shown for completeness at the bottom of Figure 1.

All the electronic structure calculations in this work are based on the DFT[46,47] implemented in the Gaussian 03 program package.[48] The structures of the stationary points on the potential energy surface were calculated employing the B3LYP hybrid functional[49−51] for the exchange and correlation energies. Geometry optimizations and single point energy calculations have been performed employing an all electron 6-31G(d,p) basis set for all the atoms in the adsorption products involving the $Si_{15}H_{16}$ and Si_9H_{12} cluster models. On the other hand, for the adsorption products involving the larger cluster model $Si_{31}H_{32}$, the geometry optimizations have been performed by employing the 6-31G(d,p) basis set only for benzene and first- and second-layer silicon atoms, while a LanL2DZ basis set with pseudopotentials for the core electrons was used for the third- and fourth-layer silicon atoms. On these optimized structures, single point energy calculations have been carried out employing the 6-31G(d,p) basis set for all the atoms. To assess the reliability of the 6-31G(d,p) basis set, a larger 6-311+G(d,p) basis set was employed to perform single point energy calculations on the main stationary points of the energy surface for the C−H breaking on the two smallest Si_9H_{12} and $Si_{15}H_{16}$ clusters, paths a and b in Scheme 1 and on the other adsorption configurations. The results show that at B3LYP level the two basis sets give very similar values, the differences being less than 3.0 kcal mol^{-1} (see below). Binding energies and binding enthalpies at 0 K, including the zero point energy corrections, have been evaluated for the stationary points with respect to free reactants (silicon cluster models and benzene) at infinite distance. The B3LYP functional has been used extensively in the past few years to calculate binding and activation energies of organic reactions on Si(100) surfaces using the cluster approximation, leading to results generally in good agreement with the experiment.[52−56] The performance of B3LYP in predicting the reaction barriers and energies has been assessed against large thermochemistry and themochemical kinetics experimental databases.[57−58] These benchmarks indicate that B3LYP reproduces pretty well the reaction enthalpies and atomization energies with mean errors of 1−5 kcal mol^{-1} while systematically understimating energy barriers by 2−6 kcal mol^{-1}, depending on the basis set and the considered database. Moreover, within the considered databases, B3LYP has given more reliable results for pericyclic reactions of hydrocarbons[57] and for hydrogen transfer reactions,[58] the kind of reaction occurring on the Si(100) surface that we considered in our work. Although these mean errors are larger than the "chemical accuracy" of 1−2 kcal mol^{-1}, they are small enough to make B3LYP reliable in reproducing, though not always quantitatively, experimental data. To assess the reliability of the B3LYP approach, we performed single point calculations at the MP2 level with the large 6-311+G(d,p) basis set on the main stationary points of the energy surface for the C−H breaking on the two reduced Si_9H_{12} and $Si_{15}H_{16}$ clusters, paths a and b in Scheme 1, and at the QCISD level only on the smallest Si_9H_{12} cluster with a mixed basis set (6-311+G(d,p) for the top layer silicon atoms and benzene molecule and 3-21G for the other atoms). Unrestricted B3LYP calculations have been performed for the structures with radical and biradical character. The extent of biradical character has been estimated empirically from the magnitude of the expectation value $\langle S^2 \rangle$ from broken symmetry spin unrestricted DFT calculations.[59] The computed $\langle S^2 \rangle$ values for the stationary points with diradicaloid character have been supplied in the Supporting Information, Table 1.

Results and Discussion

A. Adsorption Products. We have considered seven bonding configurations for the adsorption of benzene on Si(100) that can undergo the C−H bond cleavage process on the sp^3 carbon atoms anchored to the surface, and they are sketched in Chart 1. In particular, **1** and **2**, respectively, correspond to the 1,2 tilted **(T)** and 1,4 butterfly (**Bf**) di-σ bonded configurations on top of a single dimer, while **3** and **4**, respectively, correspond to the **TwB** and the **TiB** tetra-σ bonded configurations, all previously characterized both experimentally and theoretically.[27−32,35] Structures **5** and **6** correspond to 1,4 butterfly di-σ bonded configurations where the benzene bridges two dimers on the same row, the former being aligned to the dimer row (bridge butterfly, **BBf**), the latter lying diagonally across the two dimers (diagonal butterfly, **DBf**). Finally, structure **7** shows a 1,4 di-σ bonded configuration, where the benzene molecule bridges two dimers on two adjacent rows through two Si−C bonds, leaving one dangling silicon atom on each dimer (bridging rows, **BR**). Even if this bonding configuration has not been identified in any experimental investigation of benzene adsorbed on Si(100), other six-membered ring systems, such as 1,3-cyclohexadiene[60] and chlorinated benzene,[37,38] have been observed to add across

CHART 1: Bonding Configurations for the Adsorption of Benzene on Si(100)

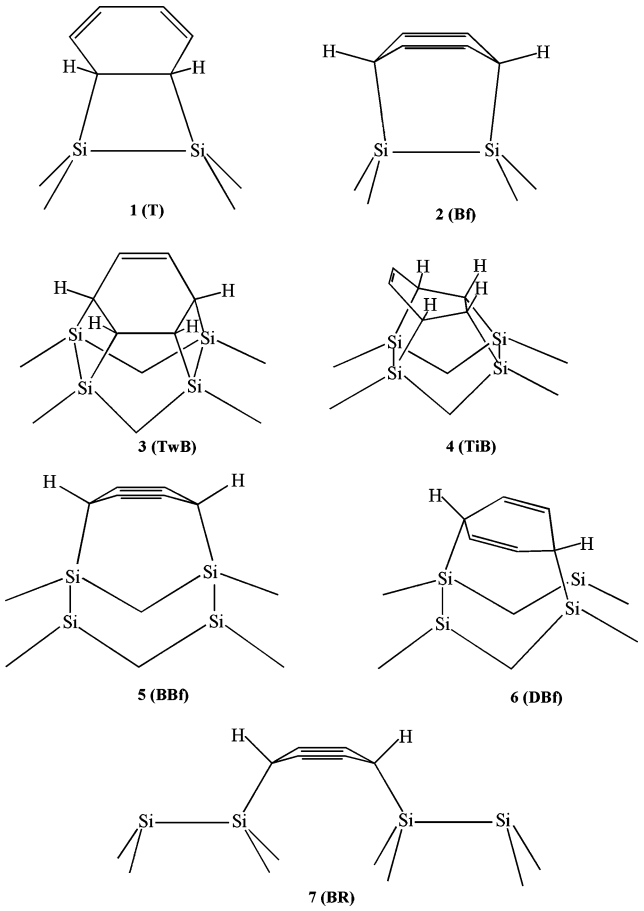

the dimer rows, and also longer acenes, such as pentacene, are found to adsorb on the silicon surface through this configuration.[40,61] Structures **5**−**7** correspond to high-energy configurations for the benzene adsorption and have not been experimentally observed; nevertheless, they could undergo a C−H bond cleavage, which is expected to involve quite high energy barriers, more easily than the low-energy configurations **2**−**4** and have been therefore considered in the present study.

Geometry optimizations have been performed for all the benzene adsorption products according to the bonding configurations depicted in Chart 1, by employing the finite cluster models described above. The computed optimized structures are reported in Figure 2, together with the main geometrical parameters, while the computed binding energies and binding enthalpies are reported in Table 1. It is worth noting that the binding enthalpies values are systematically higher than the binding energies by 1−2 kcal mol^{-1}, due to the higher contribution to the zero point energy of two more Si−C bonds in the adsorption products.

A binding enthalpy of only −4.1 kcal mol^{-1} with respect to free reactants has been computed for **1**, consistent with previous calculations performed at the same level of theory,[29] while structures **2**, **3**, and **4** are largely more stable in energy, with binding energy values of −19.0, −19.3, and −32.3 kcal mol^{-1}, respectively. As previously outlined by Gordon at a MRMP2//CASSCF level of theory,[35] the tetra-σ bonded structures **3** and **4** are overestimated in energy by single-reference DFT calculations, so that they are probably above the di-σ structure **2**. Anyway, since the four Si−C σ bonds will impart to these structures a strong rigidity, quite high energy barriers are

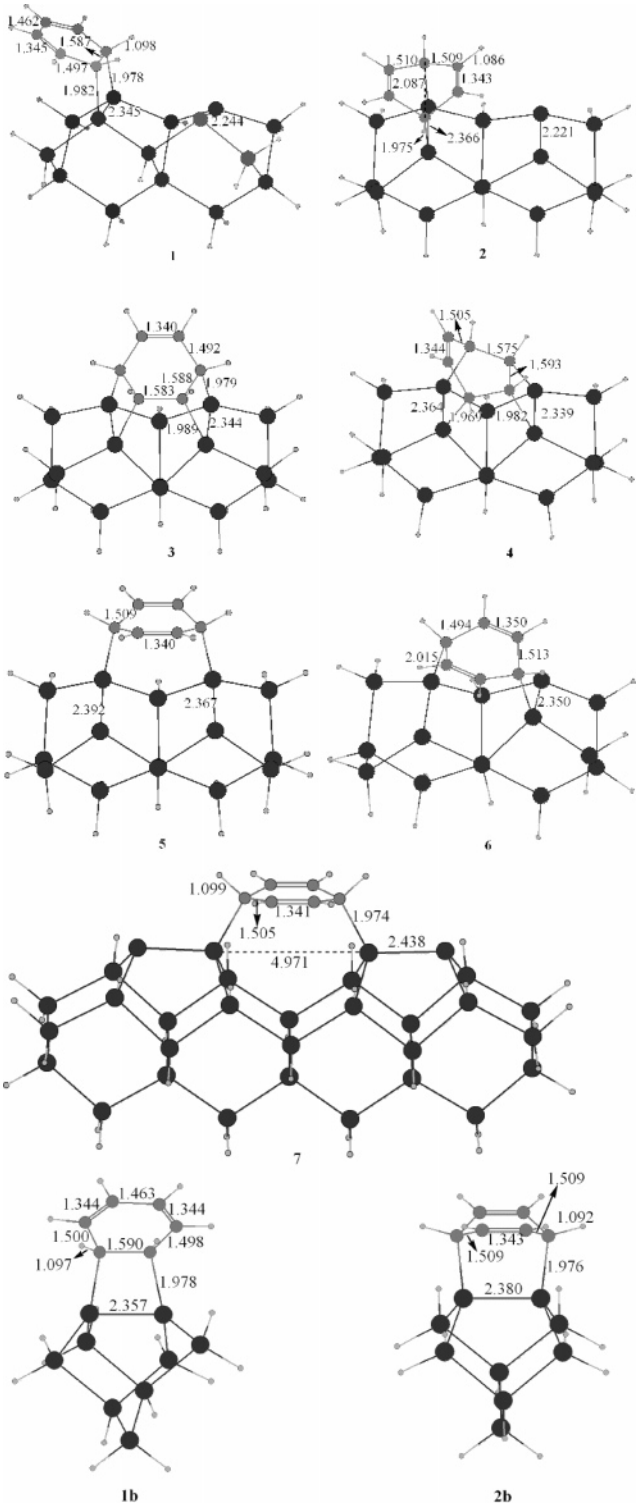

Figure 2. Optimized structures for the adsorbed benzene products on the Si(100) surface, together with the main geometrical parameters (bond lengths in ångstroms).

expected for the C−H bond cleavage process from **3** and **4**, and they have been therefore ruled out.

More attractive for the topic of our paper are the diradical structures **5**−**7**, even if they have never been identified in any experimental study of benzene adsorbed on Si(100). As it is shown in Table 1, structures **5** and **6**, both corresponding to 1,4 bonding configurations on two adjacent dimers, show quite different binding energy values, respectively, of −17.0 and +12.6 kcal mol^{-1} with respect to free reactants. The high stability of **5** can be attributed to the low distortion of the

TABLE 1: Binding Energy (ΔE) and Binding Enthalpy at 0 K (ΔH_0) (kcal mol^{-1}) at the B3LYP/6-31G(d,p) Level of Theory for Benzene Adsorption Products 1−7 Reported in Figure 2[a]

	1	1b	2	2b	3	4	5	6	7
ΔE	−4.9 (−3.6)	−4.7 (−2.9)	−20.5 (−19.1)	−21.5 (−19.9)	−21.2 (−19.3)	−34.4 (−32.5)	−18.9	+11.8	−20.0
ΔH_0	−4.1	−4.2	−19.0	−20.5	−19.3	−32.3	−17.0	+12. 6	−18.2

[a] In parentheses are the B3LYP/6-311+G(d,p) results.

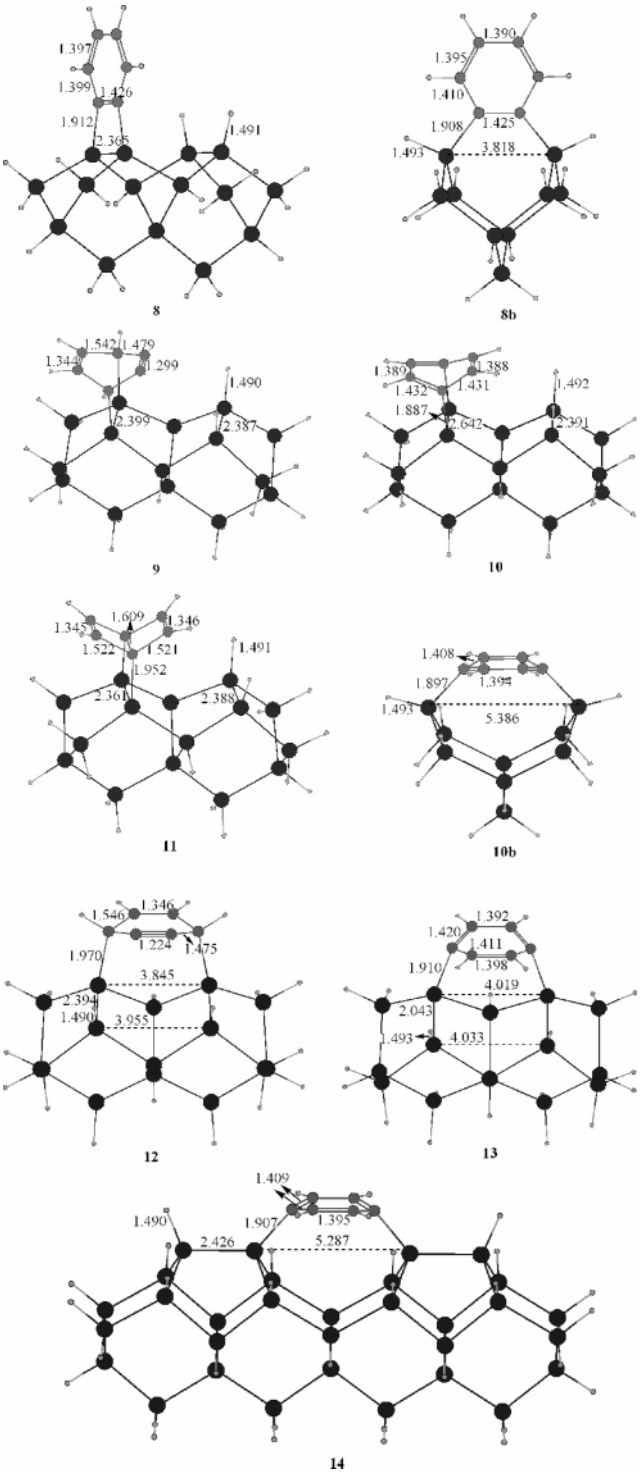

Figure 3. Optimized structures for the final products and intermediates, derived from the C−H bond cleavage on the adsorbed benzene products on the Si(100) surface, together with the main geometrical parameters (bond lengths in ångstroms).

benzene unit upon the chemisorption on the surface, since the intradimer Si−Si distances of 4.022 Å in the bare cluster model $Si_{15}H_{16}$ (see Figure 1) fits pretty well the distance of the 1,4 carbon atoms in benzene (2.793 Å). On the other hand, the high distortion of the silicon cluster upon the formation of the Si−C bonds together with the electronic repulsion between the π electron system of benzene and the unpaired electrons on the dimers can be responsible for the higher energy of **6**, which will be therefore ruled out.

Finally, structure **7**, where the benzene links two dimers on two adjacent rows, has a binding energy of −18.2 kcal mol^{-1}, a value very close to that of the experimentally detected product **2**. Indeed, in spite of the presence of two dangling silicon atoms, the adsorbed benzene in structure **7** fits well the intradimer Si−Si distance of 5.199 Å for the bare cluster model $Si_{31}H_{32}$ (see Figure 1), thus giving rise to a high thermodynamically stable configuration.

Structures **5** and **7** are calculated to be quite stable adsorption structures and only a few kilocalories per mole above the main adsorption product **2** of benzene on Si(100). The reason why they are not experimentally detected could be due to kinetic factors. Indeed, their formation is expected to proceed through a two step diradical mechanism involving two different silicon dimers and is foreseen to show a significant energy barrier, while the concerted [4+2] pathway leading to **2** is known to occur with little or no barrier.[35] In spite of this, the adsorption products **5** and **7** seem very promising for the C−H bond cleavage process, since they show two hydrogen atoms oriented toward the dangling silicon atoms and ready to undergo radical abstraction. Therefore, even if these structure are expected to be kinetically unfavorable and are not experimentally observed, they could still promote the C−H bond cleavage mechanism through low-energy channels on the potential energy surface of the adsorbed benzene.

B. C−H Bond Cleavage on the Adsorbed Benzene: Products and Their Energetics. Once we computed the minima on the potential energy surface of adsorbed benzene, we considered the thermodynamic stability of the possible products derived from the breaking of the two C−H bonds on the sp^3 carbon atoms of benzene in the adsorption configurations **1**, **2**, **5**, and **7** and the subsequent transfer of hydrogen to silicon surface atoms. Accordingly, we have identified nine minima, **8**−**14**, **8b**, and **10b**, and their optimized structures are reported in Figure 3, together with the main geometrical parameters, while the calculated binding energies and binding enthalpies with respect to free reactants are reported in Table 2. It is worth noting that the binding enthalpy values are systematically lower than the binding energies by 2−4 kcal mol^{-1}, due to the lower contribution to the zero point energy of two fewer C−H bonds in the adsorption products.

We first considered the abstraction of two hydrogen atoms from the sp^3 carbon atoms in the 1,2 bonding configuration **1**. The abstraction of the two hydrogen atoms by the dangling silicon atoms on the adjacent dimer involves a gain in energy of 62.7 kcal mol^{-1}, leading to structure **8** with a binding enthalpy of −66.8 kcal mol^{-1}, the largest among the C−H broken configurations. Indeed, in **8** the Si−C dimer bond lies in the same plane of benzene, allowing it to restore the aromaticity on the organic molecule, almost without any strain, as outlined from the computed C−C bond distances, quite close to the value

TABLE 2: Binding Energy (ΔE) and Binding Enthalpy at 0 K (ΔH_0) (kcal mol^{-1}) at the B3LYP/6-31G(d,p) Level of Theory for the Benzene Adsorption Products upon the C−H Bond Cleavages, 8−14, Reported in Figure 3[a]

	8	8b	9	10	10b	11	12	13	14
ΔE	−64.6 (−62.1)	−39.9 (−36.6)	+24.9	+12.0	−5.1	+20.4	+16.2	−17.5	−48.9
ΔH_0	−66.8	−42.2	+21.0	+8.6	−7.5	+16.3	+12.4	−20.1	−50.4

[a] In parentheses are the B3LYP/6-311+G(d,p) results.

SCHEME 1: Potential Energy Diagrams for the C−H Bond Cleavage Mechanisms on Adsorption Products 1 (Section a), 1b (Section b), and 7 (Section c), Respectively, Leading to Structures 8, 8b, and 14

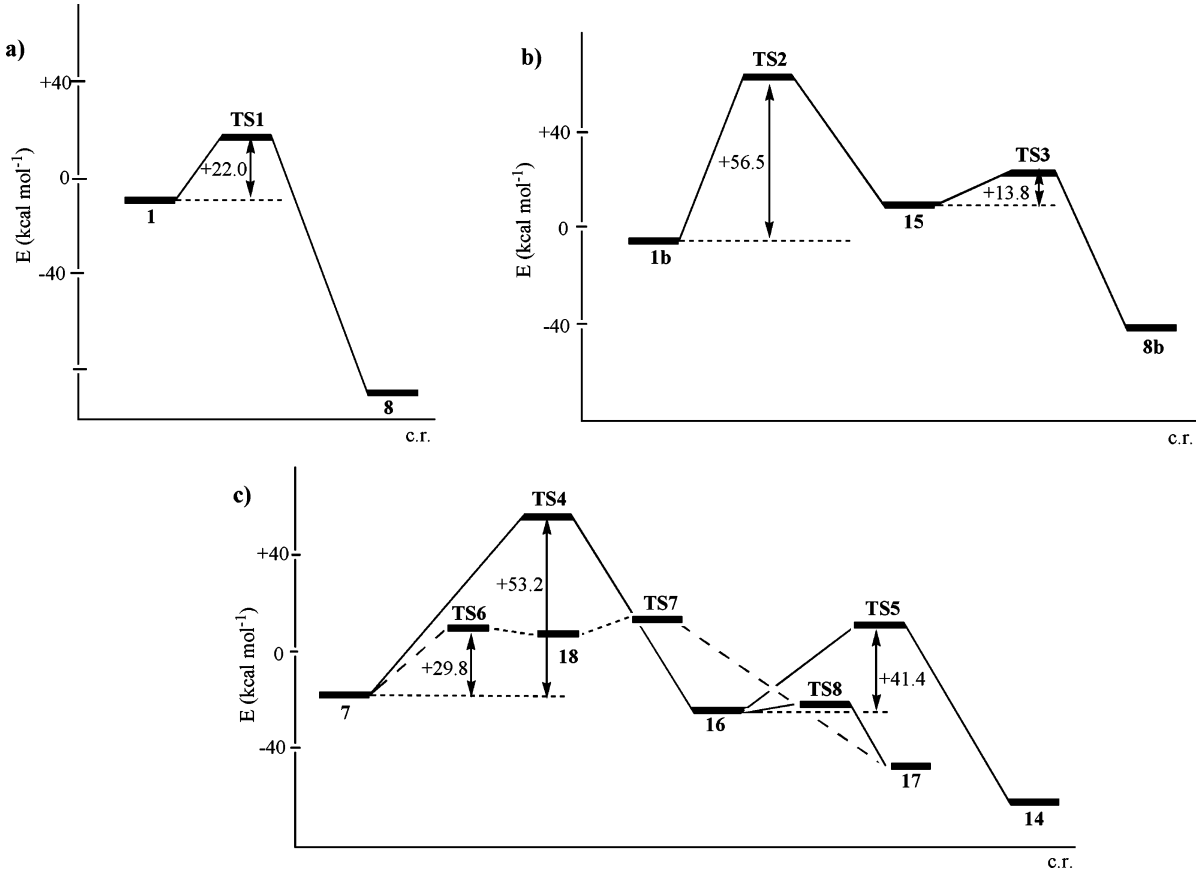

of free benzene (1.390 Å). Although the Si−Si dimer bond underlying the benzene moiety (2.365 Å) enforces a slight deviation from the sp^2 hybridization on the two carbon atoms bound to the dimer, as indicated from the outer C−C−Si angles values of 135.9°, this is the only C−H broken configuration where the silicon atoms bonding the benzene moiety lie in its plane, thus giving it a high thermodynamic stability. We also considered the possibility that the two Si−H bonds could be formed by the same silicon atoms binding benzene in **1**, along with the breaking of the underlying Si−Si dimer bond. Since only one silicon dimer is effectively involved in this process, we employed the reduced cluster model Si_9H_{12} to optimize the structure described above, **8b** in Figure 3. We also optimized the 1,2 adsorption product of benzene by employing the single-dimer cluster model, finding structure **1b** in Figure 2, that, with a binding enthalpy of −4.2 kcal mol^{-1}, is in excellent agreement with the corresponding structure **1**, computed employing the two-dimer cluster model, thus confirming the validity of reduced cluster models for the description of localized interactions on the silicon surface. The computed binding enthalpy of **8b**, −42.2 kcal mol^{-1}, shows that the cleavage of the C−H bonds leading from **1b** to **8b** involves a stabilization of only 38.0 kcal mol^{-1} and that **8b** is 24.6 kcal mol^{-1} higher in energy than **8**. The lower thermodynamic stability of **8b** with respect to **8** can be attributed to the loss of the Si−Si bond energy that, however, would imply a greater energy loss, of about 50 kcal mol^{-1}. A deeper inspection of the optimized structure **8b** reveals that the breaking of the Si−Si dimer bond allows a relaxation of the angles around the carbon atoms bounded to the surface, reaching for the outer C−C−Si angles values of 112.9°, closer to the ideal value of 120.0° than for structure **8** (135.9°). This implies for **8b** an extra stability with respect to **8**, due to a major contribution of the aromaticity to the stability of the system, of about 25 kcal mol^{-1}.

We then analyzed the hydrogen abstraction from the sp^3 carbon atoms in the 1,4 bonding configurations **2**, **5**, and **7**. The simplest reaction pathway for di-σ bonded product **2** would proceed in two steps, the first one involving the abstraction of the hydrogen atoms closer to the dangling silicon atoms and leading to the formation of metastable benzyne intermediate **9**, lying 40.0 kcal mol^{-1} above **2** (21.0 kcal mol^{-1} above reactants), which could then evolve to final product **10** via two 1,2 hydrogen shifts from the silicon bound sp^3 carbon atoms to the adjacent sp carbon atoms. Although all the carbon atoms in benzene have retained an sp^2 hybridization, the energy of the system increases 27.6 kcal mol^{-1} upon passing from **2** to **10**, since the benzene moiety is constrained on the top of the Si−Si dimer bond (2.666 Å in the free cluster model), with a high strain energy. We also verified the thermodynamic stability of the bi-cyclobutene (Dewar benzene) isomer **11**, obtainable via

the formation of a 1,4 C−C bond after the C−H bonds breaking, that lies 35.3 kcal mol^{-1} above **2** (7.7 kcal mol^{-1} above **10**), essentially due to the loss of aromaticity and to the strain energy following the formation of the 1,4 C−C bond together with the rearrangement to a bicyclobutene structure. However, comparing the thermodynamic stability of free benzene and free bicyclobutene, we computed an energy difference of 116.5 kcal mol^{-1}, which is much higher than the energy difference between **10** and **11** (7.7 kcal mol^{-1}), thus suggesting that, in spite of the loss of aromaticity, the bicyclobutene isomer pretty well fits the adsorption on the silicon surface. For the di-σ bonded **Bf** configuration **2**, we also considered the hydrogen abstraction from the sp^3 carbon atoms by the underlying silicon atoms, along with the breaking of the Si−Si dimer bond. By employing a single-dimer cluster model, we obtained the minimum structure **10b** (see Figure 3), lying only 13.0 kcal mol^{-1} higher in energy than adsorption product **2b** (see Figure 2), corresponding to structure **2**, computed employing a two-dimer cluster model. It is remarkable that **10b** is 16.1 kcal mol^{-1} lower in energy than **10**, in spite of the breaking of the Si−Si dimer bond, probably due to the reduced strain energy of the benzene moiety, which may relax to an almost planar configuration.

For 1,4 bonding configuration **5**, where the benzene bridges two adjacent dimers on the same row, we considered that the detachment of the hydrogen atoms by the silicon surface may occur in two steps, analogous to those discussed above for **2**. The first step involves the abstraction of the two adjacent hydrogen atoms lying almost above the dangling silicon atoms and leading to the metastable benzyne intermediate **12**, 29.4 kcal mol^{-1} above **5** (12.4 kcal mol^{-1} above reactants). The second step involves two hydrogen 1,2 shifts from the silicon bound sp^3 carbon atoms to the adjacent benzyne sp carbon atoms and leads to the final structure **13**, with a binding energy of −20.1 kcal mol^{-1}. Although **5** is almost isoenergetic with **2**, the corresponding products of the C−H bond cleavage, respectively **13** and **10**, showing the same number of Si−H and Si−C bonds, have quite different thermodynamic stabilities, with **13** being more stable than **10** by 28.7 kcal mol^{-1}. Also in this case, the driving force for the energy of the system after the C−H bond breaking is the attainment of the planarity of the benzene moiety, which is favored by a longer distance between the benzene-bound silicon atoms, i.e., 4.019 Å in **13** versus 2.642 Å in **10**.

Finally, the 1,4 bonding **BR** configuration **7**, with the benzene linking two dimers on two adjacent rows, can evolve to structure **14**, which, with a binding enthalpy of −50.4 kcal mol^{-1}, is the second thermodynamically most stable C−H broken structure (see Table 2). The optimized structure of **14** shows that the Si−Si distance of 5.287 Å between the dimer rows still fits quite well the 1,4 C−C distance of 2.820 Å in benzene, so that the benzene moiety may relax to an almost planar structure with sp^2 carbon atoms, leading to an energy gain of 32.2 kcal mol^{-1} with respect to **7**.

The binding energies of the minima on the potential energy surface for the adsorption of benzene on the silicon surface and for the breaking of two C−H bonds, restoring the sp^2 hybridization on all the carbon atoms, indicate that this dissociation process is thermodynamically favored only for the 1,2 adsorption products **1** (−4.1 kcal mol^{-1}), leading to structure **8** (−66.8 kcal mol^{-1}) or **8b** (−42.2 kcal mol^{-1}), and for the 1,4 bonding configuration **7** (−18.2 kcal mol^{-1}), leading to structure **14** (−50.4 kcal mol^{-1}).

C. Kinetics of the C−H Bond Cleavage Mechanism on the Adsorbed Benzene. We finally analyzed the kinetics of the C−H bond cleavage for the adsorption configurations **1** and **7**, leading to the thermodynamically most stable products, looking for the transition states connecting the adsorption configurations to the final C−H broken structures containing the two Si−H bonds. The potential energy diagrams for the C−H bond cleavage mechanisms for the adsorption products **1** (**1b**) and **7**, leading to the structures **8** or **8b** and **14**, respectively, have been outlined in Scheme 1. We identified on these potential energy surfaces a total of eight transition states, **TS1**−**TS8**, and four further minima, **15**−**18**, and their optimized structures are reported in Figure 4, together with the main geometrical parameters, while the calculated binding energies and binding enthalpies are reported in Table 3. According to Scheme 1a, we found only one transition state, **TS1**, connecting **1** to **8**, lying 22.0 kcal mol^{-1} above **1** (17.9 kcal mol^{-1} above free reactants). The structure of **TS1** in Figure 4 shows that this transition state corresponds mainly to the transfer of one hydrogen atom, while the transfer of the second hydrogen atom is essentially barrierless. The optimized structure of **TS1** reported in Figure 4 shows that one C−H bond is very lengthened (1.476 Å), and correspondingly, a Si−H bond is forming (1.779 Å), while also the second C−H is slightly lengthened (1.171 Å) with respect to the equilibrium value, so that it is ready for the abstraction by the close dangling silicon atom, which occurs without any energy barrier. We also considered the energy barrier for the [2+2] adsorption product **1**, computing an activation energy of 11.0 kcal mol^{-1} above free reactants, which correspond to an activation energy of 15.9 kcal mol^{-1} for the benzene desorption from **1**. These results compare quite well with recent calculations at UB3LYP and multireference MP2 level of theory with a different basis set,[35] showing an activation energy of, respectively, 11.5 and 8.9 kcal mol^{-1} for the [2+2] cycloaddition (22.0 and 18.7 kcal mol^{-1} for the corresponding desorption process).

On the other hand, according to Scheme 1b, two transition states, **TS2** and **TS3**, connected by an intermediate, **15**, have been identified on the reaction pathway leading from **1b** to **8b**. The first C−H bond breaking involves a high energy barrier (56.5 kcal mol^{-1} above **1b**, i.e., 52.3 kcal mol^{-1} above free reactants), while the breaking of the second C−H bond is energetically much easier, with an activation energy of 13.8 kcal mol^{-1} above **15** (27.2 kcal mol^{-1} above free reactants). The abstraction of the first hydrogen atom leads to the formation of a metastable biradical intermediate **15** (13.4 kcal mol^{-1} above free reactants), characterized by the formation of only one Si−H bond formed along with the breaking of Si−Si dimer bond (3.942 Å), while the abstraction of the second atom represents a low-energy channel to reach a high gain in energy, through the attainment of the aromaticity in the final product **8b**. The optimized structure for **TS2** shows a lengthening of the C−H bond (1.743 Å), while a Si−H bond on the underlying silicon atom is forming (1.722 Å) and the Si−C bond is shortened (1.880 Å) to promote the abstraction of the hydrogen atom. On the other hand, in **TS3** structure the first Si−H bond has already formed, while the carbon to silicon transfer of the second hydrogen atom is occurring: the C−H is lengthened (1.387 Å), and the Si−H bond is forming (1.564 Å).

To check the reliability of the 6-31G(d,p) basis set and of the B3LYP level of theory for the considered surface processes, single point calculations with the large 6-311+G(d,p) basis set at B3LYP and MP2 levels were performed on the main stationary points of the energy surface for the C−H breaking on the two reduced Si_9H_{12} and $Si_{15}H_{16}$ clusters, paths a and b in Scheme 1 and at the QCISD level on the smallest Si_9H_{12} cluster with a mixed basis set (6-311+G(d,p) for the top layer silicon atoms and benzene molecule and 3-21G for the other

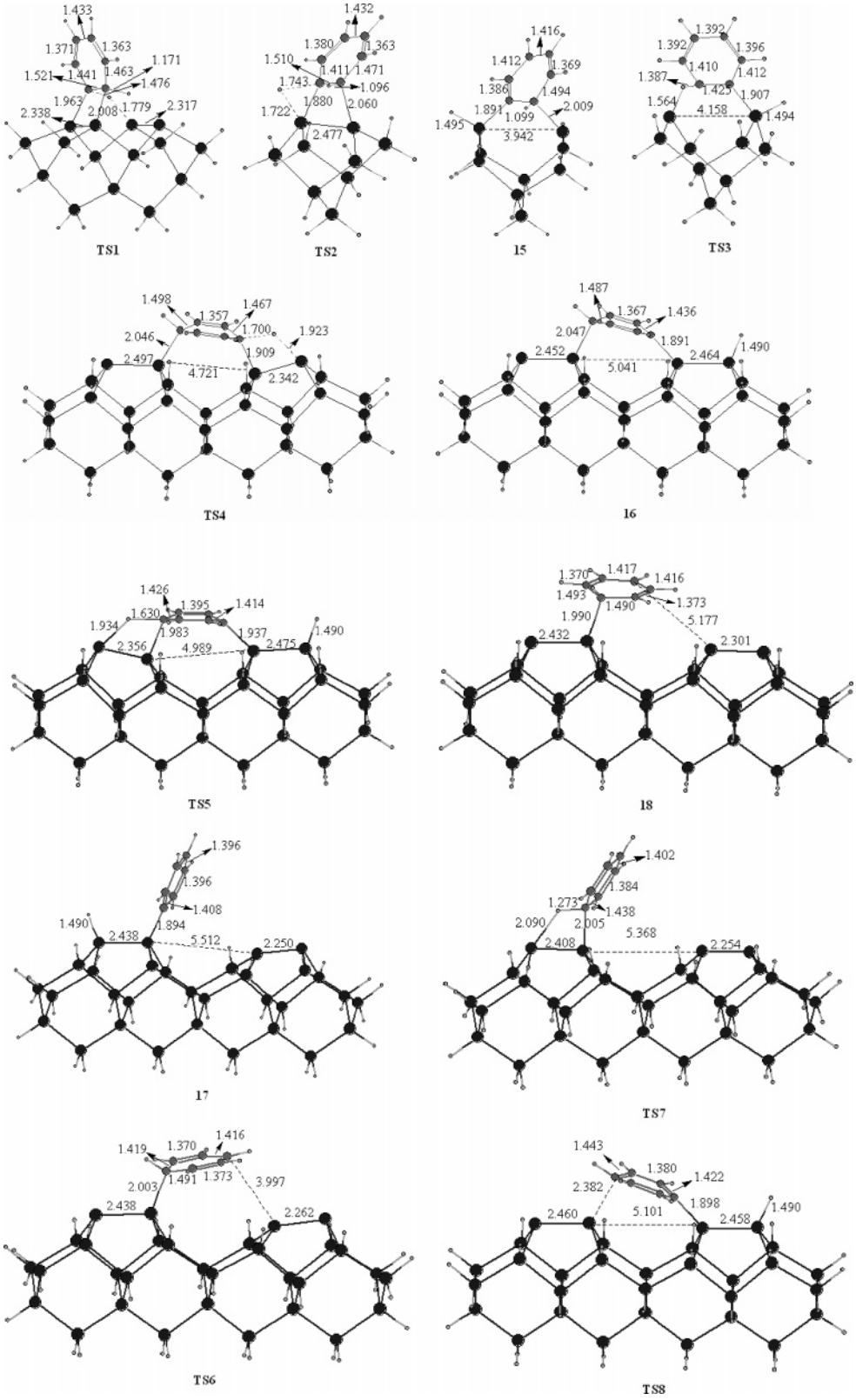

Figure 4. Optimized structures for the transition states and intermediates along the C−H bonds cleavage pathways for the adsorbed benzene products on the Si(100) surface, together with the main geometrical parameters (bond lengths in ångstroms).

atoms). The results show that at B3LYP level the two basis sets give very similar values, the differences being less than 3.0 kcal mol^{-1} (see Tables 1−3). The MP2 calculations also show a good agreement with the DFT level of theory. In particular, we estimated a reaction energy of −57.6 and of −30.1 kcal mol^{-1} at the MP2 level (−58.5 and −33.7 kcal mol^{-1} at B3LYP level), respectively, for the C−H bond breakage process from **1** to **8** and from **1b** to **8b**, while an activation energy of 18.5 and 64.6 kcal mol^{-1} has been estimated at the MP2 level (26.6 and 61.5 kcal mol^{-1} at B3LYP level), respectively, for the **TS1** and **TS2** structures. Furthermore, the QCISD calculations on the smallest Si_9H_{12} cluster give for the C−H bond

TABLE 3: Binding Energy (ΔE) and Binding Enthalpy at 0 K (ΔH_0) (kcal mol^{-1}) at the B3LYP/6-31G(d,p) Level of Theory for Transition States TS1−TS8 and Intermediates 15−18 Involved in the Computed C−H Bond Cleavage Processes[a]

	TS1	TS2	TS3	TS4	TS5	TS6	TS7	TS8	15	16	17	18
ΔE	+21.4 (23.0)	+57.1 (58.6)	+32.0 (34.7)	+38.5	+16.6	+11.9	+18.6	−20.9	+15.6 (17.9)	−22.7	−44.8	+10.9
ΔH_0	+17.9	+52.3	+27.2	+35.0	+17.7	+11.6	+15.7	−22.2	+13.4	−23.7	−45.3	+10.0

[a] The structure label refer to Figure 4. In parentheses are the B3LYP/6-311+G(d,p) results.

process from **1b** to **8b** a reaction energy value (−24.6 kcal mol^{-1}) and an activation energy value for **TS2** (70.6 kcal mol^{-1}) in reasonable agreement with the MP2 calculations.

When we considered the reaction pathway leading from **7** to **14**, we found two transition states (**TS4** and **TS5**) and one intermediate, **16**, connecting them. The rate determining step of this reaction pathway involves the C−H bond cleavage of the first hydrogen atom and passes through the transition state **TS4**, lying 53.2 kcal mol^{-1} above **7** (35.0 kcal mol^{-1} above free reactants). The optimized geometry of **TS4** shows a distortion of both the benzene molecule and the silicon dimer abstracting the hydrogen atom. The C−H bond is lengthened up to 1.700 Å, while the forming Si−H bond is still long, 1.923 Å, and the Si−C bond is shortened to 1.909 Å to promote the abstraction of the hydrogen. Once the Si−H bond has formed, **TS4** relaxes to the biradical intermediate **16**, where the benzene moiety is tilted toward the formed Si−H bond and one of the two unpaired electrons has shifted from one of the dangling silicon atom to the neighbor carbon atom. Due to the hydrogen abstraction, one of the two sp^3 carbon atoms of benzene has reached an sp^2 hybridization, and the resulting radical benzene moiety is stabilized by the configuration of the unpaired electron with the two double bonds, so that the energy of **16** is 5.5 kcal mol^{-1} below that of **7** (23.7 kcal mol^{-1} below free reactants). The abstraction of the second hydrogen atom passes through **TS5** and involves a lower energy barrier of 41.4 kcal mol^{-1} above **16** (17.7 kcal mol^{-1} above free reactants) leading to the final product **14**, where the aromaticity of benzene has been fully restored. The optimized structure of **TS5** shows the incipient abstraction of the second hydrogen atom, with a lengthened C−H bond of 1.630 Å and a forming Si−H bond of 1.934 Å. In a recent theoretical study of the dissociative adsorption of chlorinated benzene on Si(100), Polanyi et al.[38] considered for comparison the C−H bond cleavage for the **BR** adsorption configuration and computed for the transition states **TS4** and **TS5** slightly higher values, respectively, of 69 and 46 kcal mol^{-1} at a B3LYP/6-31G*//HF/3-21G level of theory.

We also identified another minimum on the potential energy surface from **7** to **14**, i.e., structure **17** in Figure 4, where one Si−H bond has formed and one Si−C bond has broken on the opposite side, thus leading to a vertical phenyl unit anchored to the surface. This structure, where the aromaticity has been completely restored, lies 45.3 kcal mol^{-1} below free reactants, i.e., only 5.1 kcal mol^{-1} higher in energy than **14**. We then considered the reaction pathway leading from the adsorbed configuration **7** to structure **17**, finding two transition states, **TS6** and **TS7**, connected by an intermediate, **18**. The metastable intermediate **18** is reached from **7** through the rupture of one of the two Si−C bonds and is a slightly endothermic process (+10.0 kcal mol^{-1}) with a very late transition state (**TS6**), barely above the product (1.6 kcal mol^{-1}), as expected for a bond breaking process. Such an intermediate is a diradical species, with an sp^3 carbon atom σ-bonded to one dimer silicon atom and with one unpaired electron on the adjacent silicon, while the other one is partially delocalized on the benzene ring. It easily relaxes to **17** passing through the transition state **TS7**, which shows the incipient rupture of the C−H bond (1.273 Å) and the incipient formation of the Si−H bond (2.090 Å). Interestingly, adsorption product **17** can also be reached from intermediate **16** by means of a lengthening of the strained Si−C bond (2.047 Å), passing through a transition state **TS8** lying only 1.5 kcal mol^{-1} above **16**. The optimized structure of **TS8** shows that the Si−C has been almost completely broken (2.382 Å), so that the sp^3 carbon atom has retained the sp^2 hybridization. **TS8** easily relaxes to **17** through the complete rupture of the Si−C bond and the orientation of the phenyl unit vertically to the silicon dimer. The potential energy diagram sketched in Scheme 1c suggests that for the **BR** configuration of benzene the C−H bond cleavage pathway leading to structure **17** is expected to be kinetically more favorable than that leading to final product **14**, where two Si−H bond have formed.

Conclusions

In the present paper, we report a DFT study on the possible mechanisms for the hypothetic C−H bond cleavage process on benzene, in order to shed light on the analogous process on larger polycyclic aromatic hydrocarbons. Our calculations suggest four feasible reaction pathways for the hypothetical C−H bond cleavage on the adsorbed benzene. Among these, one of the most kinetically favored reactive channel involves the abstraction of two hydrogen atoms bound on the sp^3 carbon atoms by the silicon atoms of an adjacent dimer in the **T** configuration, passing through the transition state **TS1** (22.0 kcal mol^{-1}). Although seemingly low, such an activation energy is not expected to be accessible at temperatures below the onset of benzene desorption from this configuration, which requires 15.9 kcal mol^{-1}. Moreover, previous studies[35] highlighted that the **T** benzene configuration is metastable toward the more stable 1,4 butterfly di-σ bonding configuration (**Bf**). Another kinetically competitive reactive channel involves the rupture of one Si−C bond in the **BR** configuration, which, however, has not been experimentally detected for the benzene molecule, passing through an energy barrier of 29.8 kcal mol^{-1} (**TS6**), and ends with the formation of a Si−H bond and a vertical phenyl unit anchored on a silicon dimer (structure **17**). The remaining two reaction pathways also start from the **T** and **BR** configurations but show higher activation energies, respectively, of 56.5 and 53.2 kcal mol^{-1}.

We remark that the C−H bond cleavage processes discussed in this work have not been experimentally detected for benzene, for which a thermal desorption occurs at 460−500 K,[26] i.e., at temperatures below those required to overcome the lowest energy barrier for a C−H bond cleavage process. However, our work has given useful insights into the dissociative adsorption on the Si(100) surface of longer acenes, such as pentacene, where the molecule is anchored on the silicon surface much more strongly than benzene, through four pairs of Si−C bonds, thus preventing the desorption process and enabling dissociative events involving the rupture of some C−H bonds. In this context, we can hypothesize that the **T** and the **BR** configurations could be good candidates for the abstraction of hydrogen atoms from sp^3 carbon atoms on the adsorbed pentacene. Further investigations are still required to shed light on the reliability

of the C−H bond ruptures of longer acenes adsorbed on Si(100), and they are currently being carried out in our laboratory.

Acknowledgment. This work was supported by MIUR (FIRB 2003 "Molecular compounds and hybrid nanostructured materials with resonant and non-resonant optical properties for photonic devices") and by CNR.

Supporting Information Available: Optimized geometries and total electronic energies for all the stationary points described in this work. Computed $<S^2>$ values for the stationary points with diradicaloid character. This material is available free of charge via the Internet at http://pubs.acs.org.

References and Notes

(1) Buriak, J. M. *Chem. Rev.* **2002**, *102*, 1271.
(2) Bent, S. F. *Surf. Sci.* **2002**, *500*, 351.
(3) Hamers, R. J. *Nature* **2001**, *412*, 489.
(4) Wolkow, R. A. *Annu. Rev. Phys. Chem.* **1999**, *50*, 413.
(5) Appelbaum, J. A.; Baraff, G. A.; Hamann, D. R. *Phys. Rev.* **1976**, *14*, 588.
(6) Redondo, E.; Goddard, W. A. *J. Vac. Sci. Technol.* **1982**, *21*, 344.
(7) (a) Uda, T.; Shigekawa, H.; Sugawara, Y.; Mizuno, S.; Tochihara, H.; Yamashita, Y.; Yoshinobu, J.; Nakatsuji, K.; Kawai, H.; Komori, F. *Prog. Surf. Sci.* **2004**, *76*, 147 and references therein. (b) Jung, Y.; Shao Y.; Gordon, M. S.; Doren, D. J.; Head-Gordon, M. *J. Chem. Phys.* **2003**, *119*, 10917. Jung, Y.; Akinaga, Y; Jordan, K. D.; Gordon, M. S. *Theor. Chem. Acc.* **2003**, *109*, 268.
(8) Hamers, R. J.; Coulter, S. K.; Ellison, M. D.; Hovis, J. S.; Padowitz, D. F.; Schwartz, M. P.; Greenlie, C. M.; Russel, J. N., Jr. *Acc. Chem. Res.* **2000**, *33*, 617.
(9) Yates, J. T., Jr. *Chem. Rev.* **1995**, *95*, 1589−1673.
(10) Hovis, J. S.; Liu, H.; Hamers, R. J. *Surf. Sci.* **1998**, *402*, 1.
(11) Wang, G. T.; Mui, C.; Musgrave, C. B.; Bent, S. F. *J. Phys. Chem.* **1999**, *103*, 6803.
(12) Li, X. *J. Am. Chem. Soc*. **2003**, *125*, 6384.
(13) Lee, H. S.; Choi, C. H.; Gordon, M. S. *J. Phys. Chem. B* **2005**, *127*, 8485.
(14) Liu, X.; Zhu, M.; Wang, X. *J. Phys. Chem. B* **2004**, *108*, 7359.
(15) Festa, G.; Cossi, M.; Barone, V.; Cantele, G.; Ninno, D.; Iadonisi, G. *J. Chem. Phys.* **2005**, *122*, 184714.
(16) Rintelman, J. M.; Gordon, M. S. *J. Phys. Chem. B* **2004**, *108*, 7820.
(17) Sorescu, D. C.; Jordan, K. D. *J. Phys. Chem. B* **2000**, *104*, 8259.
(18) Taylor, P. A.; Wallce, R. M.; Cheng, C. C.; Weinberg, W. H.; Dresser, M. J.; Choyke, W. J.; Yates, J. T., Jr. *J. Am. Chem. Soc*. **1992**, *114*, 6754.
(19) Konecny, R.; Doren, D. J. *Surf. Sci.* **1998**, *417*, 169.
(20) Wang, G. T.; Mui, C.; Musgrave, C. B.; Bent, S. F. *J. Phys. Chem.* **1999**, *103*, 6803.
(21) Choi, C. H.; Gordon, M. S. *J. Am. Chem. Soc*. **1999**, *121*, 11311.
(22) Minary, P.; Tuckerman, M. E. *J. Am. Chem. Soc*. **2004**, *126*, 13920.
(23) Konecny, R.; Doren, D. J. *J. Am. Chem. Soc*. **1997**, *119*, 11098.
(24) Teplyakov, A. V.; Kong, M. J.; Bent, S. F. *J. Am. Chem. Soc.* **1997**, *119*, 11100.
(25) Minary, P.; Tuckerman, M. E. *J. Am. Chem. Soc*. **2005**, *127*, 1110.
(26) Taguchi, Y.; Fujisawa, M.; Takaoka, T.; Okada, T.; Nishijima, M. *J. Chem. Phys*. **1991**, *95*, 6870.
(27) Lopinski, G. P.; Moffatt, D. J.; Wolkow, R. A. *Chem. Phys. Lett*. **1998**, *282*, 305.
(28) Lopinski, G. P.; Fortier, T. M.; Moffat, D. J.; Wolkow, R. A. *J. Vac. Sci. Technol., A* **1998**, *16*, 1037.
(29) Wolkow, R. A.; Lopinski, G. P.; Moffatt, D. J. *Surf. Sci. Lett*. **1998**, *416*, L1107.
(30) Silvestrelli, P. L.; Ancilotto, F.; Toigo, F. *Phys. Rev. B* **2000**, *62*, 1596.
(31) Kong, M. J.; Teplyakov, A. V.; Lyubovitsky, J. F.; Bent, S. F. *Surf. Sci*. **1998**, *411*, 286.
(32) *(32) Witkowski, N.; Hennies, F.; Pietzsch, S.; Mattson, S.; Fohlish, A.; Wurth, W.; Nagasono, M.; Piancastelli, M. N. Phys. Rev. B* **2003**, *68*, 115408.
(33) Shimomura, M.; Munakata, M.; Honma, K.; Widstrand, S. M.; Johansson, L.; Abukawa, T.; Kono, S. *Surf. Rev. Lett.* **2003**, *10*, 499.
(34) Witkowski, N.; Pluchery, O.; Borensztein, Y *Phys. Rev. B* **2005**, *72*, 075354.
(35) Jung, Y.; Gordon, M. S. *J. Am. Chem. Soc*. **2005**, *127*, 3131.
(36) Li, Q.; Leung, K. T. *J. Phys. Chem. B* **2005**, *109*, 1420.
(37) Naumkin, F. Y.; Polanyi, J. C.; Rogers, D.; Hofer, W.; Fisher, A. *Surf. Sci.* **2003**, *547*, 324.
(38) Naumkin, F. Y.; Polanyi, J. C.; Rogers, D. *Surf. Sci.* **2003**, *547*, 335.
(39) Kasaya, M.; Tabata, H.; Kawai, T. *Surf. Sci.* **1998**, *400*, 367.
(40) Hughes, G; Roche, J.; Carty, D; Cafolla, T.; Smith, K. E. *J. Vac. Sci. Technol., B* **2002**, *20*, 1620.
(41) Weidkamp, K. P.; Hacker, C. A.; Schwartz, M. P.; Cao, X. P.; Tromp, R. M.; Hamers, R. J. *J. Phys. Chem. B* **2003**, *107*, 11142.
(42) Ruiz, R.; Choudhary, D.; Nickel, B.; Toccoli, T.; Chang, K.-C.; Mayer, A. C.; Clancy, P.; Blakely, J. M.; Headrick, R. L.; Iannotta, S.; Malliaras, G. G. *Chem. Mater*. **2004**, *16*, 4497.
(43) Craig, B. I. *Surf. Sci. Lett*. **1993**, *280*, 279.
(44) Widjaja, Y.; Musgrave, C. B. *Surf. Sci.* **2000**, *469*, 9.
(45) Lu, X.; Zhu, M. *Chem. Phys. Lett.* **2004**, *393*, 124 and references therein.
(46) Hohenberg, P.; Kohn, W. *Phys. Rev.* **1964**, *136*, B864.
(47) Kohn, W.; Sham, L. J. *Phys. Rev.* **1965**, *140*, A1133.
(48) Frisch, M. J.; Trucks, G. W.; Schlegel, H. B.; Scuseria, G. E.; Robb, M. A.; Cheeseman, J. R.; Zakrzewski, V. G.; Montgomery, J. A., Jr.; Stratmann, R. E.; Burant, J. C.; Dapprich, S.; Millam, J. M.; Daniels, A. D.; Kudin, K. N.; Strain, M.; Pomelli, C.; Adamo, C.; Clifford, S.; Ochterski, J.; Petersson, G. A.; Ayala, P. Y.; Cui, Q.; Morokuma, K.; Malick, D. K.; Rabuck, A. D.; Raghavachari, K.; Foresman, J. B.; Cioslowski, J.; Oritz, J. V.; Stefanov, B. B.; Liu, G.; Liashenko, A.; Piskorz, P.; Komaromi, I.; Gomperts, R.; Martin, R. L.; Fox, D. J.; Keith, T.; Al-Laham, M. A.; Peng, C. Y.; Nanayakkara, A.; Gonzalez, C.; Challacombe, M.; Gill, P. M. W.; Johnson, B. G.; Chen, W.; Wong, M. W.; Andres, J. L.; Head-Gordon, M.; Replogle, E. S.; Pople, J. A. Gaussian 03; Gaussian Inc.: Pittsburgh, PA, 1998.
(49) Becke, A. D. *J. Chem. Phys.* **1993**, *98*, 1372.
(50) Becke, A. D. *J. Chem. Phys*. **1993**, *98*, 5648.
(51) Lee, C.; Yang, W.; Parr, R. G. *Phys. Rev. B* **1988**, *37*, 785.
(52) Mui, C.; Bent, S. F.; Musgrave, C. B. *J. Phys. Chem. A* **2000**, *104*, 2457.
(53) Barriocanal, J. A.; Doren, D. J. *J. Phys. Chem. B* **2000**, *104*, 12269.
(54) Widjaja, Y.; Mysinger, M. M.; Musgrave, C. B. *J. Phys. Chem. B* **2000**, *104*, 2527.
(55) Nunzi, F.; Sgamellotti, A.; Re, N. *J. Phys. Chem. B* **2004**, *108*, 10881.
(56) Nunzi, F.; Sgamellotti, A.; Re, N. *J. Phys. Chem. B* **2006**, *110*, *7682*.
(57) Guner, V.; Khuong, K. S.; Leach, A. G.; Lee, P. S.; Bartberger, M. D.; Houk, K. N. *J. Phys. Chem. A* **2003**, *107*, 11445.
(58) Kang, J. K.; Musgrave, C. B. *J. Chem. Phys.* **2001**, *115*, 11040. Zhao, Y.; Truhlar, D. G. *J. Phys. Chem. A* **2004**, *108*, 6908. Zhao, Y.; Truhlar, D. G. *J. Phys. Chem. A* **2005**, *109*, 5656. Zhao, Y.; Schultz, N. E.; Truhlar, D. G. *J. Chem. Theory Comput.* **2006**, *2*, 364.
(59) Hrovat, D. A.; Duncan, J. A.; Borden, W. T. *J. Am. Chem. Soc.* **1999**, *121*, 169.
(60) Teague, L. C.; Boland, J. J. *J. Phys. Chem.* **2003**, *107*, 3820.
(61) Choudhary, D.; Clancy, P.; Bowler, D. R. *Surf. Sci.* **2005**, *578*, 20.